J.Natn.Sci.Foundation Sri Lanka 2022 50 (2): 467 - 475
DOI: http://dx.doi.org/10.4038/jnsfsr.v50i2.10666

RESEARCH ARTICLE

Nanomedicine

Effect of PEGylated gold nanorods on the circulating vascular endothelial growth factor, platelet-derived growth factor, and miR-29a in CD-1 mice

AM Gamal-Eldeen[1*], BM Raafat[2], CA Fahmy[3,4], MT Abo-Elfadl[3,4], SM El-Daly[4,5] and MRK Ali[6]

[1] *Clinical Laboratory Sciences Department, College of Applied Medical Sciences, Taif University, Taif 21944, Saudi Arabia.*
[2] *Radiological Sciences Department, College of Applied Medical Sciences, Taif University, Taif 21944, Saudi Arabia.*
[3] *Biochemistry Department, National Research Centre, 33 El Buhouth St. Dokki, Cairo, 12622, Egypt.*
[4] *Cancer Biology and Genetics Laboratory, Centre of Excellence for Advanced Sciences, National Research Centre, 33 El Buhouth St. Dokki, Cairo, 12622, Egypt.*
[5] *Medical Biochemistry Department, National Research Centre, 33 El Buhouth St. Dokki, Cairo, 12622, Egypt.*
[6] *Advanced Material Sciences and Nanotechnology Laboratory, Center of Excellence for Advanced Sciences, National Research Centre, Dokki, Cairo, 12622, Egypt.*

Submitted: 25 August 2021; Revised: 05 February 2022; Accepted: 25 February 2022

Abstract: Gold nanorods (GNRs) show promising biomedical therapeutic/imaging applications. This study investigated the effect of PEGylated-GNRs on the angiogenesis factors: vascular endothelial growth factor (VEGF) and platelet derived growth factor (PDGF) and their regulator (miR-29a-3p) under variable administration conditions—dosage, gender, routes of administration, and post-treatment intervals. In CD-1 mice of both genders, PEG-GNRs (94, 375, 750, and 1500 ng/kg body weight, ~40 nm, aspect ratio ~4.5) were injected via different routes: intravenous, subcutaneous, and intramuscular, and then VEGF and PDGF were estimated in sera by ELISA, after post-treatment intervals (1, 3, and 7 days). Low doses of PEG-GNRs (94 and 375 ng/kg body weight) resulted in anti-angiogenic effects, while the highest dose (1500 ng/kg body weight) provoked a pro-angiogenic effect, especially in females and with intravenous route. The expression of miR-29a was significantly diminished in intravenous (IV) and intramuscular (IM) groups at day 7, in both males and females. miR-29a may be responsible for the increased VEGF in the highest PEG-GNRs dose, but it is not responsible for the inhibited VEGF and PDGF levels in low PEG-GNRs doses. The study recommends the consideration of the critical role of dose, gender, and route of administration in PEG-GNRs pro-angiogenic activity, in medical applications as a direct cancer therapy and as a drug delivery agent.

Keywords: Angiogenesis, gender, gold nanorods, miR-29a-3p, routes of administration, VEGF and PDGF.

INTRODUCTION

Gold nanoparticles (GNPs) have emerged as a promising candidate for photothermal therapy (PTT) and imaging agents for biomedical applications (Bansal *et al.*, 2020). Depending on the GNP's size, structure, and the suspension media, a narrow range of light frequencies stimulate the resonant conduction band electron oscillation. Rod-shaped gold nanoparticles (GNRs) have two surface plasmon bands resulting from the coherent electron oscillations (Kang *et al*., 2020). The transverse plasmon band of GNRs occurs at ~520 nm. The longitudinal plasmon and much stronger band at longer wavelengths is controlled by the GNRs ratio of length and width (aspect ratio). GNRs of variable dimensions have been prepared which absorb within ~800–1200 nm, a range covering the biological water window, where water does not absorb, a diminished background fluorescence occurs, limited chromophores absorb, and consequently

* Corresponding author (aeldeen7@yahoo.com; https://orcid.org/0000-0002-4423-5616)

light can penetrate deeper into biological tissues. Those characteristics provide a promising clinical application and support the recommendation of GNR as a biomedical therapeutic/imaging agent (Bansal *et al*., 2020).

In biological systems, the aggregates of GNRs regulate their affinity to cross cell membranes and to interact with cells (Okoampah *et al.*, 2020). Additionally, plasma comprises electrolytes and proteins that can modulate the active surface charge of GNRs and their state of aggregation. GNRs can be functionalized with poly(ethylene) glycol (PEG), a surface coat that is frequently used to prevent both the adsorption of GNRs to non-specific proteins and the aggregation of GNRs (Okoampah *et al*., 2020). PEG-GNRs possess a strong surface plasmon band that provides fluorescence, absorption, and light scattering in the near-infrared (NIR) region and NIR induced-luminescence (Zong *et al.*, 2021). Accordingly, PEG-GNRs have been proved as contrast agents for *in vivo* bioimaging and as plasmonic PTT (PPTT) agents, via their efficient conversion of the absorbed light energy into heat (Mantri & Jokerst, 2020).

Angiogenesis, the development of new blood capillaries from current vessels, is essential for the growth and progression of tumours (Lugano *et al.*, 2020). Tumours cannot expand larger than a certain size (1–2 mm), as a result of deficiencies of oxygen and critical nutrients (Akbarpour Ghazani *et al.*, 2020). Accretion of inflammatory infiltrates and fibrosis provokes tissue resistance to the blood flow and accordingly oxygen delivery. Under these conditions, angiogenesis arises, dominating the upregulation of pro-angiogenic factors that stimulate the vascular remodelling and the development of new vessels (Alkilany & Murphy, 2010). Vascular endothelial growth factor (VEGF) and platelet derived growth factor (PDGF) are essential inflammatory angiogenesis promoters (Alkilany & Murphy, 2010). They bind to cell surface receptors that enhance the release of plasminogen activators and proteases, which degrade the basement membrane. This degradation stimulates cells to migrate, multiply, and differentiate into lumen-containing capillaries (Alkilany & Murphy, 2010). Measuring the angiogenic factors and their receptors in serum provides an important tool to follow-up cancer progression.

The inhibition of angiogenesis has been reported as a potential therapeutic modality for cancers, by abolishing their oxygen and nourishment supply and by preventing further proliferation and metastasis (Alkilany & Murphy, 2010; Lugano *et al.*, 2020). Many angiogenesis inhibitors have been discovered as potential treatments in various pathological angiogenesis-mediated disorders; one of these is GNPs. Although studies have reported the varied biomedical uses of PEG-GNRs in sensing, imaging, PTT of cancer, antibody-targeting (Pan *et al.*, 2009), and drug delivery (Huang *et al*., 2006), in addition to investigating the cytotoxicity and genotoxicity in cells (Abo-Zeid *et al*., 2015a, b; Gamal-Eldeen *et al.*, 2016), no studies, to our knowledge, have explored the effect of PEG-GNRs in angiogenesis. Since VEGF and PDGF are essential cytokines for angiogenesis induction, the aim of this study is to investigate the influence of different routes of administration [intravenous (IV), subcutaneous (SC), and intramuscular (IM) injections], gender (male and female), PEG-GNRs dose (94–1500 ng/kg body weight), and post-treatment intervals (1, 3, and 7 days) on the circulating pro-angiogenic growth factors (VEGF and PDGF) and on their regulator (miR-29a-3p) in CD-1 mice.

MATERIALS AND METHODS

Materials

Male and female wild type CD-1 mice (5–6 weeks old; 18–20 g; n = 520) were divided into 26 groups (20 mice/group) (Theodor Bilharz institute, Cairo, Egypt) and maintained under controlled conditions (24°C, a 12 h light/dark cycle, drinking water and feed *ad libitum*) (UCCMA feed mill factories, Cairo, Egypt). After 10 d of acclimatization, mice experiments were performed, adhering to the guidelines for animal care of the Ethical Committee, National Research Centre, Cairo, Egypt, and followed the guidelines of National Institutes of Health (USA) for the animal care and use. Chemicals were purchased from Aldrich and Fisher, USA, unless mentioned.

Preparation of PEG-GNRs

Preparation of PEG-GNRs was carried out using the seed-mediated growth method described elsewhere (Nikoobakht & El-Sayed, 2003; Abo-zeid *et al.*, 2015b). The absorption spectrum of PEG-GNRs solution was measured using a Jasco UV-vis-near-infrared spectrophotometer, V-630. A JEOL JEM-100CXII Transmission electron microscope (TEM) type JEOL-JSGM T1230 was used to examine the morphology and particle size of the prepared nanoparticles. Quantitative gold analysis was estimated by ICP mass spectrometry (Tang *et al.*, 2020), using an Agilent 7500c (Agilent, Tokyo, Japan). Dilutions and concentrations of PEG-GNRs solution were precisely measured, spectrophotometrically.

Animal experiments

In order to compare the effect of gender, dose, and route of administration of the PEG-GNRs on angiogenesis factors, 3.75, 15, 30, and 60 ng Au/100 µL injection volume were administrated to CD-1 mice in physiological saline (equivalent to 94, 375, 750, and 1500 ng/kg body weight) by IV, SC and IM routes of administration. Each experiment included its corresponding control group (saline-administrated). These doses were selected according to a preliminary clearance study, under publication, which indicated that PEG-GNRs remained in tissues after seven days from the treatment and we selected 5% of LD50 (31.2 mg/kg body weight) to be the highest dose to use, with no adverse effects. Mice of 1500 ng/kg body weight were sacrificed after 1, 3 and 7 days of injections, while mice groups of other doses were sacrificed after 7 days post-injection. One mL of the blood was collected from the caudal vein of each mouse, using a restrainer, after immersion in 0.75% Bupivacaine, as a topical anaesthetic, for 30 s. After mice scarification, sera were obtained by centrifugation of mice blood at 3000 rpm/min at 4°C for 15 min, aliquoted and stored at - 80°C until analysis.

Evaluation of angiogenesis factors

Serum levels of VEGF and PDGF-BB of the 26 groups were evaluated by quantitative Solid Phase Sandwich ELISA using Mouse Quantikine ELISA Kit (R&D Systems, Minneapolis, MN), according to the manufacturer's instructions. Colour intensity was measured at 450 nm by a microplate reader (FLUOstar OPTIMA, BMG LABTECH GmbH, Offenburg, Germany).

Expression of miR-29a-3p

Total RNA including miRNA were extracted from the sera of mice (miRNeasy Serum/Plasma Kit; #217184; Qiagen, USA). In qRT-PCR analysis, cDNA was reverse-transcribed (miScriptII RT kit; #218061; Qiagen). The hsa-miR-29a-3p miRCURY LNA miRNA PCR Assay (YP00204698, Qiagen), similar to mmu-miR-29a-3p, was applied with miScript SYBR Green PCR Kit (#218073, Qiagen). The qRT-PCR protocol included 95°C for 10 min, followed by 40 cycles of 95°C for 10 s and 60°C for 60 s. RNU6B expression, endogenous normalization control, was analysed. Changes in Ct values (Ct) between RNU6B and miRNA were submitted for the relative expression calculations, the $2^{-\Delta\Delta CT}$ method, using this formula: (ΔΔCt = ΔCt of the tested sample − ΔCt of the control sample). The relative miRNA expression was calculated by ΔΔCt protocol (Livak & Schmittgen, 2001), after normalization to U6 expression of control.

Statistical analysis

Statistical analyses were performed using SPSS version 22 (SPSS, Inc., Chicago, IL). The normality was assessed using the Shapiro-Wilk test. Data were normally distributed and presented as (means ± SE). Comparisons between different groups were carried by one-way analysis of variance, followed by *post hoc* Tukey test. Correlations between variables were estimated using Pearson's correlation test. The level of significance was set at $p < 0.05$.

RESULTS AND DISCUSSION

A tumour initiates as a nonvascular mass of host-derived cells which multiply atypically. Intratumoral hypoxia occurs when the tumour grows far from the maximum effusion area of nearby vessels (around 200 µm) (Lacal & Graziani, 2018). To confront hypoxia, tumour cells create new capillaries to sustain their needs, a mechanism that is strictly similar to normal angiogenesis (Nussenbaum & Herman, 2010). However, the walls of these abnormal capillaries are regularly made of endothelial cells (ECs) and tumour cells. VEGF is an important regulator of both vasculogenesis and angiogenesis, where it is capable of exciting microvascular EC propagation, enhance EC migration, as well as inhibiting EC apoptosis, and encouraging the development of new capillaries from preexisting vessels (Nussenbaum & Herman, 2010). High levels of VEGF and its receptor VEGFR-2 have been detected in several cancers. The diminution of VEGF signalling results in a dramatic drop in the tumour vascularity (Lacal & Graziani, 2018).

Characterization of PEG-GNRs

As indicated in Figure 1a, the prepared PEG-GNRs exhibited dual-absorption bands. The first band is at 530 nm. This band corresponds to the electrons perpendicular to the long rod axis and the so-called transverse plasmon absorption. The other absorption band appears at a lower energy end at 840 nm, corresponding to PEG-GNRs with an aspect ratio of ≥ 4.5. Figure 1b showed the TEM graph of PEG-GNRs that corresponds to the absorption spectrum shown in Figure 1a. The sizes of the prepared PEG-GNRs are relatively uniform, with an average diameter of 8–9 nm, a length of 35–42 nm, and an aspect ratio of about 4.5. The higher extinction ratio of the longitudinal surface plasmon resonance peak to the transverse one, suggests that the percentage of PEG-GNRs in the solution is enormously high.

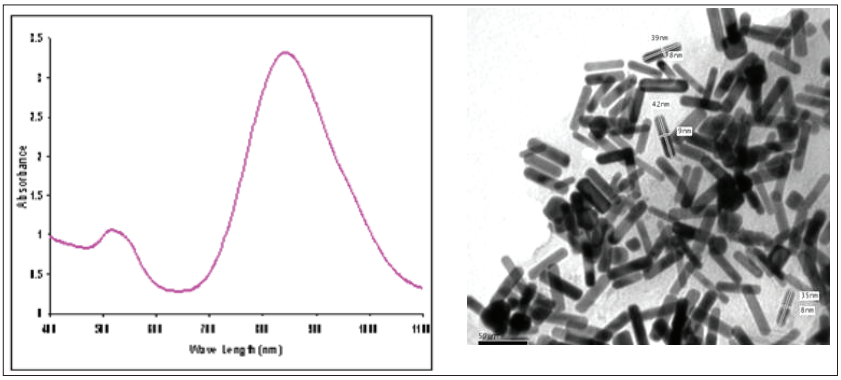

Figure 1: a. Ultraviolet-visible (UV-vis) extinction spectra of PEG-GNRs solutions. b. TEM images of PEG-GNRs

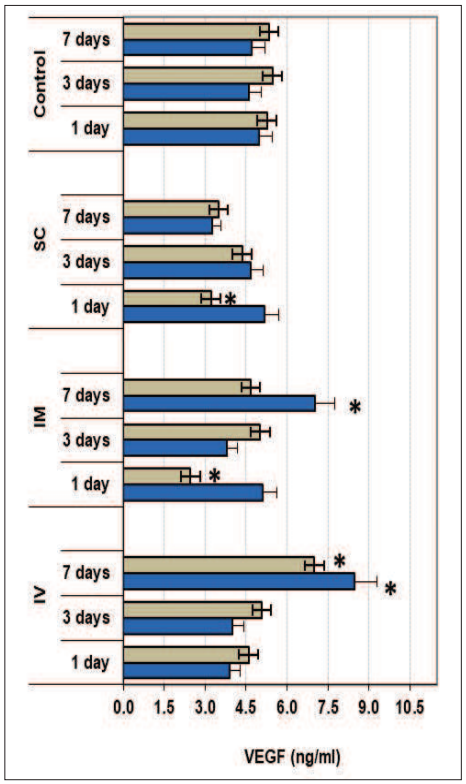

Figure 2: The effect of post-treatment intervals (1, 3, and 7 days) on serum VEGF concentration: female (blue bars) and male (grey bars) CD-1 mice were injected with PEG-GNRs (1500 ng/kg body weight) via intravenous (IV), subcutaneous (SC), and intramuscular (IM) routes. The results are expressed as mean ± standard error. * $p < 0.05$; statistically significant from control mice.

Evaluation of vascular endothelial growth factor in sera

To investigate the influence of the administration routes, gender, and PEG-GNRs doses on the circulating pro-angiogenic growth factors in CD-1 mice, the effect of post-treatment interval on VEGF concentration was firstly investigated. Mice were treated with PEG-GNRs (1500 ng/kg body weight) using different routes of administration and then sacrificed after different intervals (1, 3, and 7 days). Among these groups, IV treatment induced serum VEGF ($p < 0.05$) in both genders only after 7 days (Figure 2). IM groups showed a significant VEGF induction ($p < 0.05$) only in females after 7 days, however a significant inhibition ($p < 0.05$) was observed in males after 1 day (Figure 2), compared to their corresponding controls. In SC groups, no change was observed in VEGF in females (Figure 2), while in males an inhibited VEGF was noticeable after one day. A high positive correlation coefficient was recorded between males and females VEGF in IV groups ($r = 0.988$), while there was no correlation between males and females in IM and SC groups.

As shown in Figure 3c, after 7 days post-injection, only the highest dose led to a highly significant elevation ($p < 0.01$) in VEGF in both genders, while low doses (94 and 375 ng/kg body weight) led to a significant reduction ($p < 0.05$) in VEGF only in IV males (Figure 3a). IM groups showed a significant VEGF reduction ($p < 0.05$) in males and females treated with low doses (94 and 375 ng/kg body weight), as shown in Figure 3b. The sharp increase in PEG-GNRs dose to 1500 ng/kg

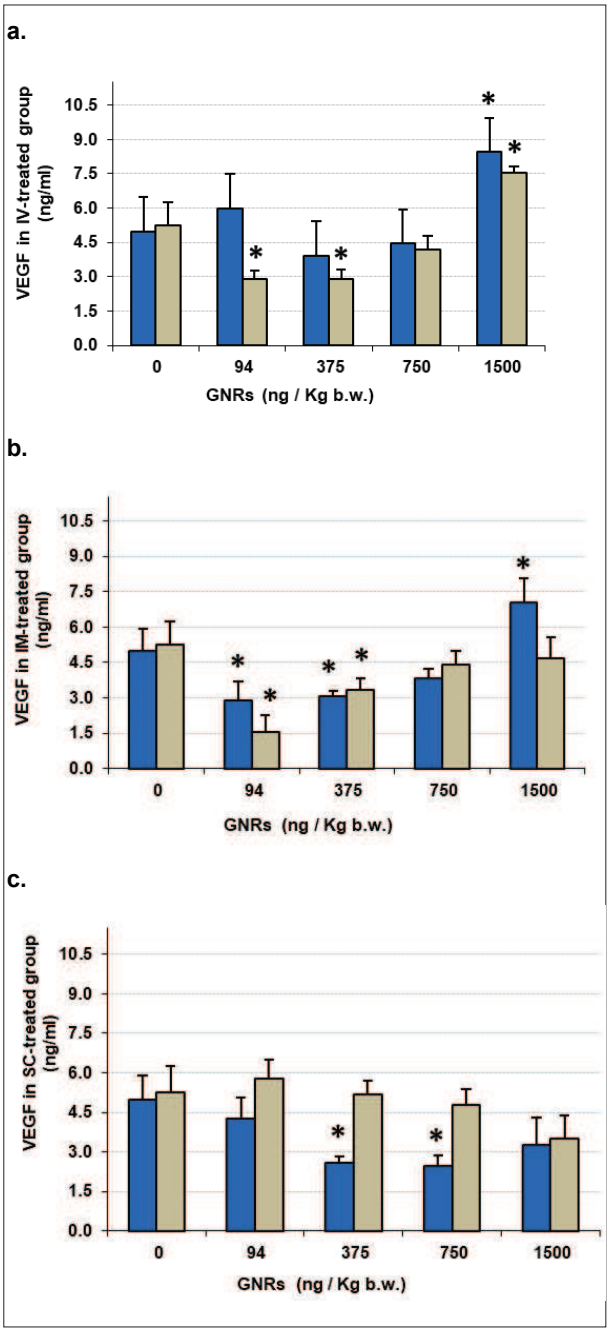

Figure 3: Effect of the administration routes, dose and gender on serum VEGF, after seven days of injection: Female (blue bars) and male (grey bars) CD-1 mice were injected with PEG-GNRs (0–1500 ng/kg body weight) via intravenous (IV) (a), intramuscular (IM) (b), and subcutaneous (SC) (c) routes. Results are expressed as mean ± standard error. *p <0.05 and **p < 0.01; statistically significant from control mice.

body weight led to a high VEGF induction in females ($p < 0.05$) (Figure 3b). No change was found among all tested doses in SC male, while in females, the doses 375 and 750 ng/kg body weight suppressed VEGF levels ($p < 0.05$), Figure 3c.

Although there is a lack of studies of the effect of GNR on VEGF, several studies investigated the effect of other nanogold shapes as promising anti-angiogenic agents. The Mukherjee group has reported that naked GNP spheres inhibit angiogenesis through their binding to heparin-binding growth factors (including bFGF and VEGF165) and inhibit their activity (Mukherjee *et al*., 2005; Bhattacharya & Mukherjee, 2008). The Pan group and Arvizo group have reported that GNP spheres significantly suppress the angiogenesis and growth of liver cancer cells and inhibit VEGF165-induced signalling (Pan *et al*., 2009; Arvizo *et al*., 2011). These data suggest that the inhibitory outcome of naked GNPs spheres results from their direct binding to VEGF165, which may be the same mechanism as GNRs, a suggestion that needs more investigation. In another study, Karthikeyan *et al.* (2010) have reported that big-size spheres (300 nM) noticeably block VEGF- and IL-1β-induced Src phosphorylation, cell growth, migration, and spreading of bovine retinal pigment epithelial cells. These reports support our findings that GNRs inhibit angiogenesis through suppressing VEGF, at low GNRs doses.

Evaluation of platelet-derived growth factor in sera

PDGF is another essential multi-role proangiogenic signalling molecule. It was initially purified from platelets; however, it has been recognized in ECs, astrocytes fibroblasts, and variable cell types. ECs express PDGF-BB receptors, and in case of receptor stimulation, an elevated DNA synthesis and angiogenic emergent can be detected. Pericytes (PCs) alleviate blood capillaries through cell-to-cell contact, and secrete PDGF (Thijssen *et al.*, 2018). Growth and migration of PCs, at the growing capillary are essentially stimulated by the interaction with PDGF (Thijssen *et al.*, 2018). Mice bred without PDGF-BB or its receptor display a dramatic elevation in the permeability of blood vessels, and they eventually died prenatally (Nussenbaum & Herman, 2010). It has been hypothesized that preventing PDGF from binding to its receptor will inhibit the growing stability of capillaries and prevent the delivery of nutrients to cancer cells (Nussenbaum & Herman, 2010).

In the current study, the effect of the post-treatment interval on PDGF concentration was investigated. Mice were treated with the highest PEG-GNRs dose. In IV males, a significant induction in serum PDGF ($p < 0.01$) was detected after all intervals, while in females PDGF was induced only after 7 days ($p < 0.01$) (Figure 4). An insignificant change in serum PDGF in IM groups observed after 1 and 3 days (Figure 4), while after 7 days, females and males had high PDGF levels ($p < 0.05$ and $p < 0.01$, respectively).

Surprisingly, in SC groups early after day 1 and day 3 of PEG-GNRs injection, PDGF showed a significant induction ($p < 0.01$) in females only, which decreased further after 7 days, whereas in males, the 7th day showed a significant elevation in PDGF ($p < 0.01$) (Figure 4). A direct correlation was found between the PDGF of males and females in both IV and IM groups ($r = 0.840$ and 0.999, respectively). However, a reverse correlation was found between males and females PDGF in SC groups ($r = -0.997$).

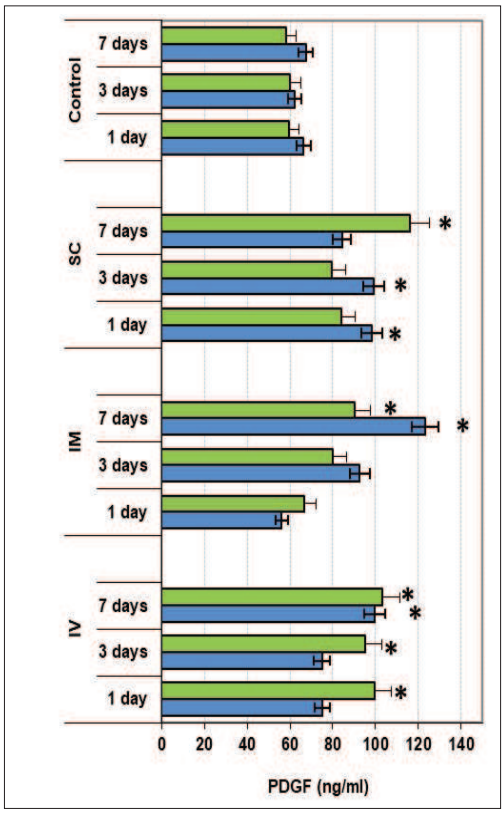

Figure 4: The effect of post-treatment intervals (1, 3, and 7 days) on serum PDGF concentration: female (blue bars) and male (green bars) CD-1 mice were injected with PEG-GNRs (1500 ng/kg body weight) via intravenous (IV), subcutaneous (SC), and intramuscular (IM) routes. The results are expressed as mean ± standard error. * $p < 0.05$ and ** $p < 0.01$; statistically significant from control mice.

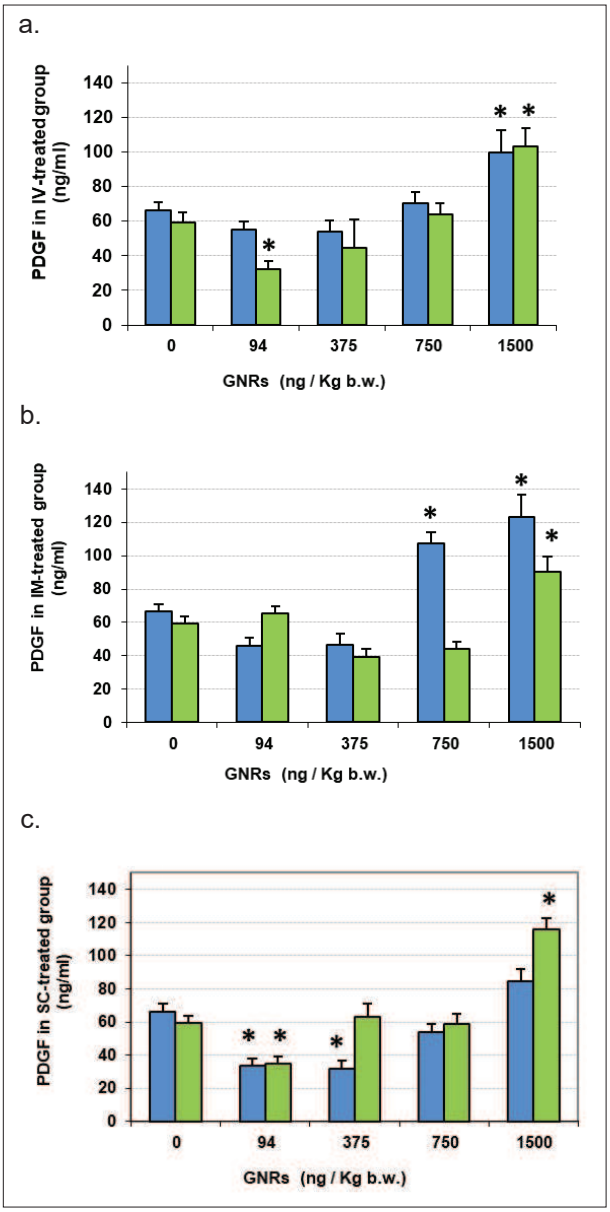

Figure 5: The effect of the administration routes, dose, and gender on serum PDGF, after seven days of injection: Female (blue bars) and male (green bars) CD-1 mice were injected with PEG-GNRs (0–1500 ng/kg body weight) via intravenous (IV) (a), intramuscular (IM) (b), and subcutaneous (SC) (c) routes. The results are expressed as mean ± standard error. *$p < 0.05$ and **$p < 0.01$; statistically significant from control mice.

The effect of dosage of PEG-GNRs on serum PDGF concentration was investigated using different doses and routes including IV- (Figure 5a), IM- (Figure 5b) and SC- (Figure 5c). After 7 days, IV injection of 1500 ng/kg body weight dramatically elevated PDGF ($p < 0.01$) in both genders (Figure 5a), while 94 ng/kg body weight inhibited PDGF ($p < 0.05$) in males (Figure 5a). PDGF displayed a significant elevation ($p < 0.01$ and $p < 0.05$) in females at high doses (750 and 1500 ng/kg body weight respectively), and in males only at 1500 ng/kg body weight, in the IM group (Figure 5b). In SC males treated with 94 ng/kg body weight, PDGF was reduced ($p < 0.05$), whereas 1500 ng/kg body weight of PEG-GNRs remarkably elevated PDGF ($p < 0.01$), (Figure 5c). In SC females, a noticeable inhibition ($p < 0.01$) of PDGF was observed at low doses (94 and 375 ng/kg body weight), (Figure 5c).

These findings suggest that low doses are capable of suppressing intratumoral angiogenesis and that particularly SC injection is a successful route to the desired biodistribution of PEG-GNRs and to diminish angiogenesis. There is a lack of studies in the published research that investigate the *in vitro* or *in vivo* effect of the gold nanostructures on PDGF. Most of the investigations were dealing with using gold aptamer conjugation to PDGF antibodies for detecting PDGF (Wang *et al.*, 2009). Cancer cells initiate angiogenesis via PCs spreading, which releases VEGF and stimulates the expression of PDGF by PCs though PDGF itself increases VEGF secretion. PDGF-BB over-expression is associated with elevated cell growth and tumour progression (Treiber *et al.*, 2009).

Expression of circulating miR-29a

The microRNA (miRNA) family includes single-stranded, small, non-coding RNAs, ~22 nucleotides, and is widely-expressed in cells and tissues (Lin *et al.*, 2020). They function mainly post-transcriptionally, where they regulate gene expression. VEGF-A was suggested to be a potential target gene of miR-29a (Chen *et al.*, 2014). Recently, it has been reported using luciferase assays and Western blot that the results confirmed that miR-29a can suppress the endogenous expression level of VEGF-A by binding to the 3'-untranslated region of VEGF-A (Zhao *et al.*, 2020).

The influence of PEG-GNRs on the expression of mmu-miR-29a-3p, which is one of the key regulators of VEGF and PDGF was investigated. The findings indicated that miR-29a expression was diminished in the IV group at day 7 in both males and females ($p < 0.01$) as well as in SC males ($p < 0.05$) and females ($p < 0.01$), as demonstrated in Figure 6. These findings suggest that miR-29a may be responsible for the increased VEGF level in high doses of PEG-GNRs, but it is not responsible for the inhibited VEGF level in low doses. This conclusion was predicted from the non-significant change in miR-29a expression in day 1, which is in contrast with the VEGF level in Figure 2. Additionally, comparing PDGF results with the miR-29a expression indicated that the changes in PDGF level (Figure 4) were not regulated by miR-29a.

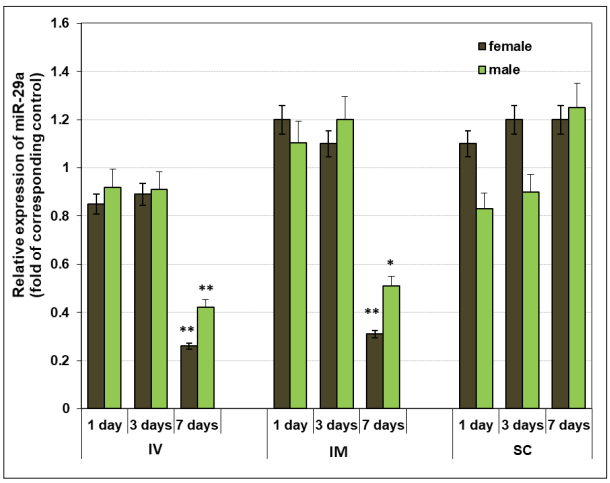

Figure 6: The effect of the administration routes, dose, and gender on the relative expression of circulating mmu-miR-29a-3p: CD-1 mice were injected with PEG-GNRs (1500 ng/kg body weight) via intravenous (IV), intramuscular (IM), and subcutaneous (SC) routes. Sera were collected from mice after 1, 3 and 7 days of injections. The results are expressed as mean ± standard error. *$p < 0.05$ and ** $p < 0.01$ compared with the corresponding control. Control expression is 1-fold.

CONCLUSION

This study is the first *in vivo* investigation of the effect of safe doses of PEG-GNRs on the pro-angiogenesis growth factors VEGF and PDGF and their regulator miR-29a, and the influence of PEG-GNRs administration conditions: dosage, gender, routes of administration, and post-administration time intervals, on both factors. Taken together, the study's findings highlight the following conclusive remarks:

- Low doses (94 and 375 ng/kg body weight) resulted in

anti-angiogenic effects.
- The highest dose of PEG-GNRs (1500 ng/kg body weight) provoked pro-angiogenic effects.
- The intravenous route resulted in pro-angiogenic effects more than other routes.
- Females exhibited more pro-angiogenic effects than males.
- miR-29a is suggested to be responsible for VEGF increase at high dose.
- Anti-angiogenic low doses can be used in PPTT of cancer.
- Consideration should be taken with high doses, especially in the bioaccumulation and clearance studies of therapeutic doses.
- Special considerations should be taken regarding the influence of dose, gender, route of administration, and post-treatment intervals.

Acknowledgement

This work was supported by Taif University Researchers Supporting Project (Number TURSP-2020/103) and National Research Centre, Cairo, Egypt.

Conflict of interest

The authors declare no conflict of interest.

REFERENCES

Abo-Zeid M.A.M., Liehr T., Gamal-Eldeen A.M., Zawrah M., Ali M. & Othman M.A.K. (2015a). Potential of rod, sphere and semi-cube shaped gold nanoparticles to induce cytotoxicity and genotoxicity in human blood lymphocytes in vitro. *European Journal of Nanomedicine* **7**: 63–75. DOI: https://doi.org/10.1515/ejnm-2014-0031

Abo-zeid M.A.M., Liehr T., Gamal-Eldeen A.M., Zawrah M. & Ali M. (2015b). Detection of cyto- and genotoxicity of rod-shaped gold nanoparticles in human blood lymphocytes using comet-FISH. *Cytologia* **80**: 173–181. DOI: https://doi.org/10.1508/cytologia.80.173

Akbarpour Ghazani M., Nouri Z., Saghafian M. & Soltani M. (2020). Mathematical modeling reveals how the density of initial tumor and its distance to parent vessels alter the growth trend of vascular tumors. *Microcirculation* **27**(1): e12584. DOI: https://doi.org/10.1111/micc.12584

Alkilany A.M. & Murphy C.J. (2010). Toxicity and cellular uptake of gold nanoparticles: what we have learned so far? *Journal of Nanoparticle Research* **12**(7): 2313–2333. DOI: https://doi.org/10.1007/s11051-010-9911-8

Arvizo R.R., Rana S., Miranda O.R., Bhattacharya R., Rotello V.M. & Mukherjee P. (2011). Mechanism of anti-angiogenic property of gold nanoparticles: role of nanoparticle size and surface charge. *Nanomedicine: Nanotechnology, Biology, and Medicine* **7**(5): 580–587. DOI: https://doi.org/10.1016/j.nano.2011.01.011

Bansal S.A., Kumar V., Karimi J., Singh A.P. & Kumar S. (2020). Role of gold nanoparticles in advanced biomedical applications. *Nanoscale Advances* **2020**(2): 3764–3787. DOI: https://doi.org/10.1039/D0NA00472C

Bhattacharya R. & Mukherjee P. (2008). Biological properties of "naked" metal nanoparticles. *Advanced Drug Delivery Reviews* **60**(11): 1289–1306. DOI: https://doi.org/10.1016/j.addr.2008.03.013

Chen L., Xiao H., Wang Z.H., Huang Y., Liu Z.P., Ren H. & Song H. (2014). miR-29a suppresses growth and invasion of gastric cancer cells in vitro by targeting VEGF-A. *BMB Reports* **47**(1): 39–44. DOI: https://doi.org/10.5483/bmbrep.2014.47.1.079

Gamal-Eldeen A., Abo-Zeid M., El-Daly S.M., Abo-elfadl M.T., Fahmy C.A., Ali M.R. & El-Sayed M. (2016). *In vivo* genotoxicity of gold nanorods in mouse bone marrow compared with cyclophosphamide. *Nano Biomedicine and Engineering* **8**: 306–314. DOI: https://doi.org/10.5101/nbe.v8i4.p306-314

Huang X., El-Sayed I.H., Qian W. & El-Sayed M.A. (2006). Cancer cell imaging and photothermal therapy in the near-infrared region by using gold nanorods. *Journal of the American Chemical Society* **128**(6): 2115–2120. DOI: https://doi.org/10.1021/ja057254a

Kang M.S., Lee S.Y., Kim K.S. & Han D.W. (2020). State of the art biocompatible gold nanoparticles for cancer theragnosis. *Pharmaceutics* **12**(8): 701. DOI: https://doi.org/10.3390/pharmaceutics12080701

Karthikeyan B., Kalishwaralal K., Sheikpranbabu S., Deepak V., Haribalaganesh R. & Gurunathan S. (2010). Gold nanoparticles downregulate VEGF-and IL-1β-induced cell proliferation through Src kinase in retinal pigment epithelial cells. *Experimental Eye Research* **91**(5): 769–778. DOI: https://doi.org/10.1016/j.exer.2010.09.003

Lacal P.M. & Graziani G. (2018) Therapeutic implication of vascular endothelial growth factor receptor-1 (VEGFR-1) targeting in cancer cells and tumor microenvironment by competitive and non-competitive inhibitors. *Pharmacological Research* **136**: 97–107. DOI: https://doi.org/10.1016/j.phrs.2018.08.023.

Lin H.-Y., Yang Y.-L., Wang P.-W., Wang F.-S. & Huang Y.-H. (2020). The emerging role of microRNAs in NAFLD: Highlight of MicroRNA-29a in modulating oxidative stress, inflammation, and beyond. *Cells* **9**: 1041. DOI: https://doi.org/10.3390/cells9041041

Livak K.J. & Schmittgen T.D. (2001). Analysis of relative gene expression data using real-time quantitative PCR and the 2(-Delta Delta C(T)) method. *Methods* **25**(4): 402–408. DOI: https://doi.org/10.1006/meth.2001.1262

Lugano R., Ramachandran M. & Dimberg A. (2020). Tumor angiogenesis: causes, consequences, challenges and opportunities. *Cellular and Molecular Life Sciences* **77**(9): 1745–1770. DOI: https://doi.org/10.1007/s00018-019-03351-7

Mantri Y. & Jokerst J.V. (2020). Engineering plasmonic nanoparticles for enhanced photoacoustic imaging. *ACS Nano* **14**(8): 9408–9422.
DOI: https://doi.org/10.1021/acsnano.0c05215

Mukherjee P., Bhattacharya R., Wang P., Wang L., Basu S., Nagy J.A., Atala A., Mukhopadhyay D. & Soker S. (2005). Antiangiogenic properties of gold nanoparticles. *Clinical Cancer Research* **11**(9): 3530–3534.
DOI: https://doi.org/10.1158/1078-0432.CCR-04-2482

Nikoobakht B. & El-Sayed M.A. (2003). Preparation and growth mechanism of gold nanorods NRs using seed-mediated growth method. *Chemistry of Materials* **15**: 1957–1962.
DOI: https://doi.org/10.1021/cm020732l.

Nussenbaum F. & Herman I.M. (2010). Tumor angiogenesis: insights and innovations. *Journal of Oncology* **2010**: 132641.
DOI: https://doi.org/10.1155/2010/132641

Okoampah E., Mao Y., Yang S., Sun S. & Zhou C. (2020) Gold nanoparticles–biomembrane interactions: From fundamental to simulation. *Colloids and Surfaces B: Biointerfaces* **196**: 111312.
DOI: https://doi.org/10.1016/j.colsurfb.2020.111312.

Pan Y.L., Qiu S.Y., Qin L., Cai J.Y. & Sun J.S. (2009). Nanogold inhibits angiogenesis and growth of liver cancer: experiment with mice. *Zhonghua Yi Xue Za Zhi* **89**(12): 800–804. (Chinese)

Tang X., Li B., Lu J., Liu H. & Zhao Y. (2020). Gold determination in soil by ICP-MS: comparison of sample pretreatment methods. *Journal of Analytical Science and Technology* **11**: 45.
DOI: https://doi.org/10.1186/s40543-020-00245-3

Thijssen V.L. *et al*. (15 authors) (2018). Targeting PDGF-mediated recruitment of pericytes blocks vascular mimicry and tumor growth. *The Journal of Pathology* **246**(4): 447–458.
DOI: https://doi.org/10.1002/path.5152

Treiber G., Wex T. & Malfertheiner P. (2009). Impact of different anticancer regimens on biomarkers of angiogenesis in patients with advanced hepatocellular cancer. *Journal of Cancer Research and Clinical Oncology* **135**(2): 271–281.
DOI: https://doi.org/10.1007/s00432-008-0443-x

Wang J., Meng W., Zheng X., Liu S. & Li G. (2009). Combination of aptamer with gold nanoparticles for electrochemical signal amplification: application to sensitive detection of platelet-derived growth factor. *Biosensors and Bioelectronics* **24**(6): 1598–1602.
DOI: https://doi.org/10.1016/j.bios.2008.08.030

Zhao Z., Sun W., Guo Z., Zhang J., Yu H. & Liu B. (2020). Mechanisms of lncRNA/microRNA interactions in angiogenesis. *Life Sciences* **254**: 116900.
DOI: https://doi.org/10.1016/j.lfs.2019.116900

Zong Q., Dong N., Yang X., Ling G. & Zhang P. (2021) Development of gold nanorods for cancer treatment. *Journal of Inorganic Biochemistry* **220**: 111458
DOI: https://doi.org/10.1016/j.jinorgbio.2021.111458.